

Nonlinearity of one-dimensional creep characteristics of soft clays

Qi-Yin Zhu¹ · Zhen-Yu Yin^{2,3} · Pierre-Yves Hicher³ · Shui-Long Shen⁴

Received: 10 February 2015 / Accepted: 24 July 2015 / Published online: 22 September 2015
© Springer-Verlag Berlin Heidelberg 2015

Abstract This study focuses on the quantitative description of the evolution of creep coefficient ($C_{\alpha e}$) with both soil density and soil structure under 1D compression. Firstly, conventional consolidation test results on various reconstituted clays are selected in order to investigate the evolution of $C_{\alpha e}$ with void ratio of soils, which can be described by a simple nonlinear creep formulation. Secondly, the contributions of the inter-particle bonding and debonding for soft structured clays to $C_{\alpha e}$ are analyzed based on test results on intact and reconstituted samples of the same clay. A material constant ρ , function of the bonding ratio χ , is introduced in order to quantify the contribution of the soil structure to $C_{\alpha e}$, and a nonlinear creep formulation accounting for both soil density and soil structure is finally proposed. Furthermore, the parameters

used in the formulation are correlated with Atterberg limits, allowing us to suggest a relationship between $C_{\alpha e}$, Atterberg limits and inter-particle bonding for a given soil. Finally, the validity of the proposed formulation is examined by comparing experimental and predicted $C_{\alpha e}$ values for both reconstituted and intact samples of natural soft clays. The proposed formulation is also validated by comparing the computed and measured void ratio with time on two intact clays.

Keywords Atterberg limits · Creep · Density · Destructuration · Oedometer test · Soft clays

1 Introduction

Natural soft clays exhibit significant creep under both laboratory and in situ conditions after primary consolidation [2, 3, 7, 9, 10, 15, 17, 19, 27, 29–32, 34]. In early days, this was often called “secondary consolidation.” The term “creep” is preferable because it is referred to the compression of soil skeleton under a constant loading, having nothing to do with consolidation [28]. The creep coefficient, defined as $C_{\alpha e} = \Delta e / \Delta \log t$ based on one-dimensional creep testing, is a key parameter for engineering practice and viscoplastic modeling [1, 11, 12, 26, 29, 32, 33]. Thus, it is important to evaluate this coefficient with accuracy.

Many studies on the characteristics of the creep have been carried out through one-dimensional creep tests on both reconstituted and intact natural clay samples. For reconstituted clay, the value of $C_{\alpha e}$ varies with the void ratio. For instance, Yin [27] and Yin et al. [30] formulated a nonlinear expression of $C_{\alpha e}$ function of volumetric strain and time under applied stresses considering the density or void ratio of soils. More recently, Yin et al. [34] proposed

✉ Zhen-Yu Yin
zhenyu.yin@gmail.com

¹ State Key Laboratory for Geomechanics and Deep Underground Engineering, China University of Mining and Technology, Xuzhou 221008, People’s Republic of China

² Key Laboratory of Geotechnical and Underground Engineering of Ministry of Education, Department of Geotechnical Engineering, College of Civil Engineering, Tongji University, Shanghai 200092, People’s Republic of China

³ Ecole Centrale de Nantes, GeM UMR CNRS 6183, LUNAM University, Nantes, France

⁴ Department of Civil Engineering, Shanghai Jiao Tong University, Shanghai 200240, People’s Republic of China

in a more precise way a linear decrease in $C_{\alpha e}$ with the void ratio in a double logarithm plane based on results on various reconstituted clays. For intact natural soft clays, the value of $C_{\alpha e}$ depends highly on the destructuration, as demonstrated by Karstunen and Yin [10], Leroueil et al. [15], Mesri and Godlewski [17] and Yin et al. [33], etc. Therefore, $C_{\alpha e}$ is generally not constant but dependent on both the void ratio and the soil structure (or inter-particle bonding and debonding) of soft soils. However, few studies have been devoted to a quantitative description of the nonlinear evolution of $C_{\alpha e}$ due to changes of both soil density and soil structure in natural soft clays. Furthermore, for correlating $C_{\alpha e}$ to clay physical properties (e.g., Atterberg limits), an average value or the value of $C_{\alpha e}$ corresponding to a final high stress level in conventional oedometer tests has usually been adopted. Since $C_{\alpha e}$ is not a constant, it is necessary to seek a reference value of $C_{\alpha e}$ to re-establish the correlation.

In this study, therefore, we focus on the quantitative description of the evolution of $C_{\alpha e}$ with both void ratio and soil structure under the condition of applied stresses exceeding the yield stress. For this purpose, available test results on intact and reconstituted samples of natural soft clays are selected for analyses. We also carry out conventional consolidation tests on reconstituted and intact samples of several clays for expanding our data base. The values of $C_{\alpha e}$ corresponding to liquid and plastic limits ($C_{\alpha eL}$, $C_{\alpha eP}$) are then estimated as reference values, based on which $C_{\alpha e}$ could be expressed as a function of one of the reference values $C_{\alpha ef}$ ($=C_{\alpha eL}$ or $C_{\alpha eP}$), the water content (w) and the inter-particle bonding (γ). Furthermore,

correlations could be established in order to estimate the value of $C_{\alpha e}$ from Atterberg limits for a given natural soft clay. Then, the proposed function is validated by comparing the estimated and experimental $C_{\alpha e}$ values.

2 Nonlinear creep related to soil density

2.1 Experimental evidence

Conventional consolidation tests on various soft clays with different mineral contents and Atterberg limits were selected for this study. In this section, all the selected data are based on reconstituted samples to eliminate the influence of soil structure. Some physical properties of the selected clays are summarized in Table 1. According to the chart shown in Fig. 1, the selected soils consist of low plastic clays, high plastic inorganic clays and high plastic silty clays. Since the void ratio (e) is a physical state of soils representing the soil density and the deformation potential, the $C_{\alpha e}$ values for all the selected clays are individually plotted against the void ratio in a double logarithmic plane, presented in Fig. 2. All the results show that $\log(C_{\alpha e})$ is linearly related to $\log(e)$.

2.2 Nonlinear creep formulation accounting for void ratio

The consideration of the density and void ratio has been addressed by Yin [27] based on Hong Kong marine clay. Based on the results in Fig. 2, the nonlinear creep

Table 1 Summary of creep coefficient of reconstituted clays under normally consolidated state

Clay	Depth/m	$C_{\alpha e}$	Applied stress corresponding to $C_{\alpha e}$ /kPa	m	e_0	G_s	w_L	I_P
Nanjing clay (1) [36]	7	0.007–0.011	25–1600	0.6627	1.8	2.7	44	21
Nanjing clay (2) [36]	9	0.011–0.015	200–800	0.7257	1.33	2.72	52	26
Wenzhou clay (1) [36]	4	0.013–0.021	25–1600	0.5489	1.67	2.7	60	32
Wenzhou clay (2) [36]	10	0.015–0.023	50–1600	0.5503	1.79	2.7	65	37
Lianyungang clay (1) [36]	4	0.023–0.039	25–1600	0.7013	2.3	2.74	86	55
Lianyungang clay (2) [36]	12	0.014–0.022	50–1600	0.6472	1.78	2.72	63	36
Shanghai clay (1) [16]	8.5	0.0072–0.0086	100–800	0.5464	1.02	2.64	51	24.6
Haarajoki clay [24]	5–15	0.0108–0.0668	40–640	2.1169	2.97	2.77	88	62
Suurpelto clay [24]	11	0.0117–0.0585	40–640	1.2273	2.66	2.52	80	57
Vanttila clay [33]	2.8	0.0212–0.0516	40–640	0.8205	3.35	2.7	90	60
Murro clay [10]	4	0.0184–0.0375	10–600	0.7337	1.94	2.66	88	54
HKMC [30]	Seabed	0.0054–0.0163	100–3200	1.0881	1.5	2.66	60	32
Shanghai clay (2)*	12	0.0062–0.0076	100–1600	0.4209	1.06	2.7	42.5	20
Zhoushan clay*	8	0.0058–0.0076	50–1600	0.3239	1.07	2.72	40.7	20
Kaolin*	–	0.0058–0.0062	50–1600	0.1372	1.13	2.65	40	20

e_0 initial void ratio, G_s specific gravity, w_L liquid limit, I_P plasticity index

* values from tests conducted by authors in this study

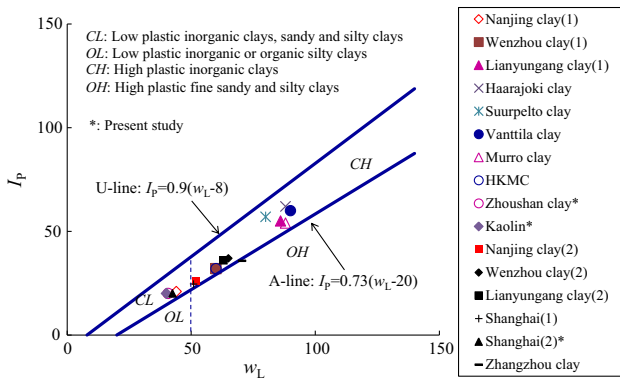


Fig. 1 Classification of soils by liquid limit and plasticity index

formulation based on Finnish clays proposed by Yin et al. [34] can be adopted:

$$C_{\alpha e} / C_{\alpha ef} = (e / e_f)^m \tag{1}$$

where $C_{\alpha ef}$ and e_f are reference values of $C_{\alpha e}$ and e , respectively (the initial in situ void ratio e_0 was used as e_f by Yin et al. [34]) and m is a material constant representing the slope of the $\log(C_{\alpha e}) - \log(e)$ curve which can be measured in a straightforward way (summarized in Table 1 for all clays). It is worth noting that $C_{\alpha e}$ is conventionally defined as the slope of the secondary compression line with the logarithm of time, which is reasonable for design purpose in civil engineering, but resulting in a negative void ratio during creep under long periods of time, whereas Eq. (1) imposes a value of e converging toward zero but remaining always positive.

The reference point ($C_{\alpha ef}$, e_f) can be arbitrary selected. However, it could be of interest to select specific values of the reference void ratio. The void ratio at the liquid or plastic limit (e_L or e_P) is usually adopted to establish the equations for compressibility [20, 21]. These two values can be easily determined from the liquid or plastic limits w_L and w_P which are usually available physical properties of clayey soils. Along these lines, two representative points (corresponding to e_L and e_P) on the $\log(C_{\alpha e}) - \log(e)$ curve can be alternatively used as reference points. Based on Fig. 2, both $C_{\alpha eL}$ and $C_{\alpha eP}$ corresponding to the void ratios e_L and e_P can be obtained and Eq. (1) can be rewritten as $C_{\alpha e} = C_{\alpha eL}(e/w_L G_s)^m$ or $C_{\alpha e} = C_{\alpha eP}(e/w_P G_s)^m$ (2)

3 Nonlinear creep related to soil structure

3.1 Experimental evidence

During conventional consolidation tests on intact samples of natural soft clays, the shape of the post-yield compression curve is significantly influenced by the debonding process during straining [10, 13, 23]. Figure 3 shows the

schematic plot of the compression curves of intact and reconstituted clay samples. For a given inelastic strain level Δe^P , the bond degradation results in the current stress σ'_v reaching point A instead of point B (assuming no destructuring). Corresponding to stress σ'_v at Δe^P , we define an intrinsic stress σ'_{vi} , which is the stress for a reconstituted sample at the same inelastic strain increment (point C). Based on this plot, a bonding ratio can be defined by $\chi = \sigma'_v / \sigma'_{vi} - 1$ with an initial bonding ratio of $\chi_0 = \sigma'_{p0} / \sigma'_{pi0} - 1$ (similar to Gens and Nova [8]; Yin et al. [33, 34]). When the strain increases, the inter-particle bonds are progressively broken and χ decreases from its initial value χ_0 toward zero, corresponding to a state where all the bonds are completely destroyed, as shown in Fig. 3.

Adopting this concept, we consider that the difference between the values of $C_{\alpha e}$ at point A and point C is due to the effect of soil structure. Defining the creep coefficients $C_{\alpha e}(I)$ and $C_{\alpha e}(R)$ at points A and C (Fig. 3), the additional creep induced by destructuring (or inter-particle debonding) can be written as:

$$\Delta C_{\alpha e} = C_{\alpha e}(I) - C_{\alpha e}(R) \tag{3}$$

3.2 Nonlinear creep formulation accounting for soil structure

To investigate the contribution of soil structure on $C_{\alpha e}$, conventional consolidation tests on both intact and reconstituted clay samples of the same clay are necessary. Table 2 summarizes the available results of 1D creep tests on both intact and reconstituted samples of ten different clays (corresponding to the first ten clays in Table 2, including the tests on Shanghai clay performed in this study). The classification of these clays is shown in Fig. 1.

Figure 4 presents the plots of $C_{\alpha e}(I)$ with the bonding ratio χ , where $C_{\alpha e}(I)$ in these graphs was directly measured from tests on intact clays. Note that $C_{\alpha e}(R)$ was estimated by Eq. (1) from experimental data on reconstituted clays at the corresponding void ratio (point C in Fig. 3) and served as the reference for the effect of destructuring. It can be seen that $C_{\alpha e}(I)$ decreases linearly with the decreasing of χ in a logarithmic scale. Based on the concept used to define χ (Fig. 3), we can express the contribution of the soil structure to the creep coefficient by the index ρ :

$$\rho = C_{\alpha e}(I) / C_{\alpha e}(R) - 1 \text{ or } \rho = \Delta C_{\alpha e} / C_{\alpha e}(R) \tag{4}$$

where ρ is always positive. In order to investigate the relation between ρ and χ , values of ρ for all the selected clays were estimated by Eq. (4) and plotted versus χ in Fig. 5. It can be observed that ρ presents a linear relationship with $\log(\chi)$, which can be expressed as:

$$\rho = n \log(\chi / \chi_0) + \rho_0 \tag{5}$$

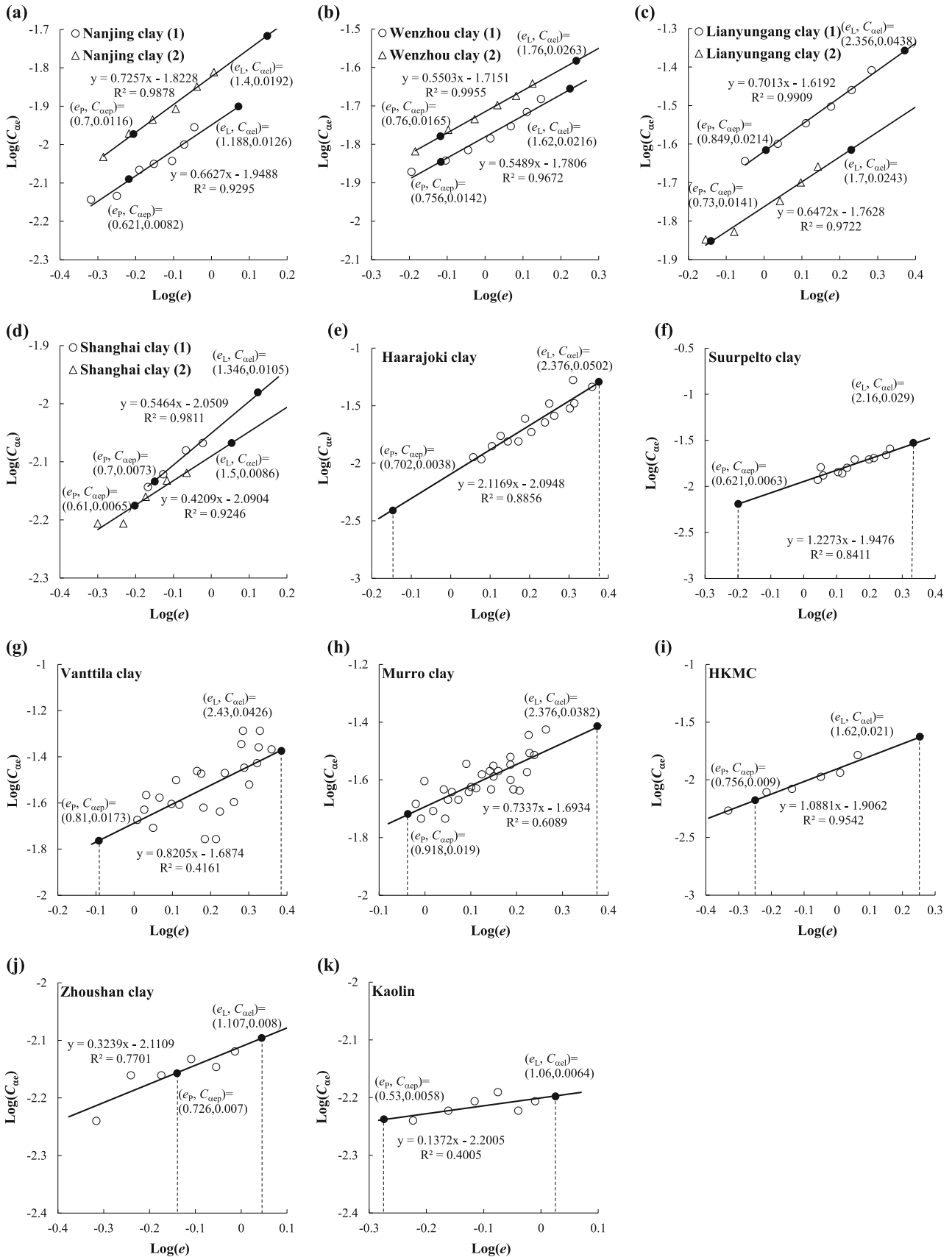


Fig. 2 Creep coefficient versus void ratio in double logarithmic scale for different reconstituted clays

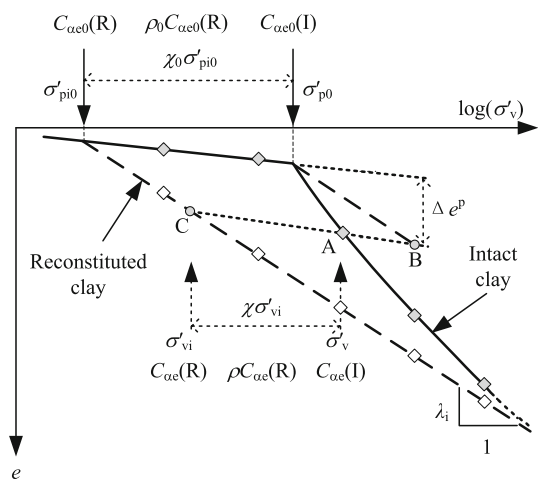


Fig. 3 Definition of the amount of inter-particle bonds

where n is a material constant representing the slope of the ρ - $\log(\chi)$ curve, ρ_0 is the initial value of ρ corresponding to $\chi = \chi_0$ and ρ decreases from ρ_0 toward zero when all the bonds are completely destroyed.

Substituting Eqs. (1) and (5) into Eq. (4), the creep coefficient for intact natural soft clays can be written as:

$$C_{\alpha e} = (n \log(\chi/\chi_0) + \rho_0 + 1) C_{\alpha ef} (e/e_f)^m \tag{6}$$

Equation (6) indicates that $C_{\alpha e}$ depends on the material constants $C_{\alpha ef}$, e_f , m , χ_0 , ρ_0 , n and the current state

variables χ and e . As described earlier, e_L or e_P can be used as e_f , and the corresponding values $C_{\alpha eL}$ or $C_{\alpha eP}$ obtained from Fig. 2 can be used as $C_{\alpha ef}$. The material constants $C_{\alpha ef}$, e_f , m can be determined from tests on reconstituted clay and χ_0 , ρ_0 , n from tests on both reconstituted and intact clays. Note that all material constants can be determined from conventional oedometer tests in a straightforward way.

The creep behavior is closely connected to the micro-properties of clay, such as the shape of particle, the inter-/intra-aggregate pore size distribution and the double layer, which can be characterized by Atterberg limits [18]. Thus, the correlations between material constants relating to creep (Eq. 6) and Atterberg limits were investigated based on available results, considering that such correlations would be useful for engineering practice.

4 Correlations of nonlinear creep properties with Atterberg Limits

4.1 Correlations of $C_{\alpha eL}$ and $C_{\alpha eP}$ with Atterberg Limits

For correlating $C_{\alpha eL}$ and $C_{\alpha eP}$ with Atterberg limits, the available test results on 15 reconstituted clays (with tests on three clays performed in this study) listed in Table 1

Table 2 Summary of creep coefficient of intact clays under normally consolidated state

Clay	Depth/m	$C_{\alpha e}$	Applied stress corresponding to $C_{\alpha e}$ /kPa	e_0	G_s	w_L	I_P	χ_0
Murro clay [10]	4	0.0163–0.0363	100–1600	2.39	2.66	88	54	22.3
Vanttila [33]	2.8	0.024–0.058	75–1200	3.4	2.7	90	60	35.2
Zhangzhou clay [37]	1.9	0.025–0.018	100–1600	1.91	2.74	70.5	35.8	8
Nanjing clay (1) [36]	7	0.009–0.019	200–1600	1.14	2.7	44	21	3.3
Nanjing clay (2) [36]	9	0.0152–0.0291	200–800	1.31	2.72	52	26.1	9.7
Wenzhou (1) [36]	4	0.021–0.049	200–1600	1.73	2.7	60	32	13.1
Wenzhou (2) [36]	10	0.016–0.040	200–1600	1.79	2.7	65	37	14.5
Lianyungang (1) [36]	4	0.024–0.055	100–800	2.2	2.74	80	49	8.6
Lianyungang (2) [36]	12	0.016–0.032	200–1600	1.78	2.72	63	36	9
Shanghai clay (2)*	12	0.01–0.017	200–1600	1.06	2.7	42.5	20	13.1
Shantou clay [35]	4.5	0.0442–0.009	100–1600	2.65	2.67	–	33	–
Guangzhou clay [6]	5	0.009–0.0076	50–100	1.25	2.7	47.5	24	–
Pusan clay [25]	–	0.1266–0.0111	320–1280	0.53–2.1	–	50–68	28–45	–
Bothkennar clay [22]	5.2	0.0454–0.0212	100–1600	–	2.65	85	48	–
Bethville clay [14]	3.2–3.5	0.023–0.115	51–135	1.73	–	46	24	–
Bastican clay [15]	7.3	0.101–0.0092	90–151	1.92	–	43	21	–
Ottawa clay [9]	–	0.0852–0.0092	200–2700	–	–	58	33	–
Leda clay [17]	–	0.0576–0.0128	30–685	–	2.74	57–60	–	–
Mexico clay [17]	38–45	0.315–0.083	80–685	–	2.35	500	350	–
New Haven clay [17]	6–26	0.1135–0.0493	25–380	–	2.68	79–97	–	–
St. Herblain clay [32]	5.7	0.193–0.020	132–515	2.29	–	96	42	–

e_0 initial void ratio, G_s specific gravity, w_L liquid limit, I_P plasticity index, χ_0 initial amount of structure

* values from tests conducted by authors in this study

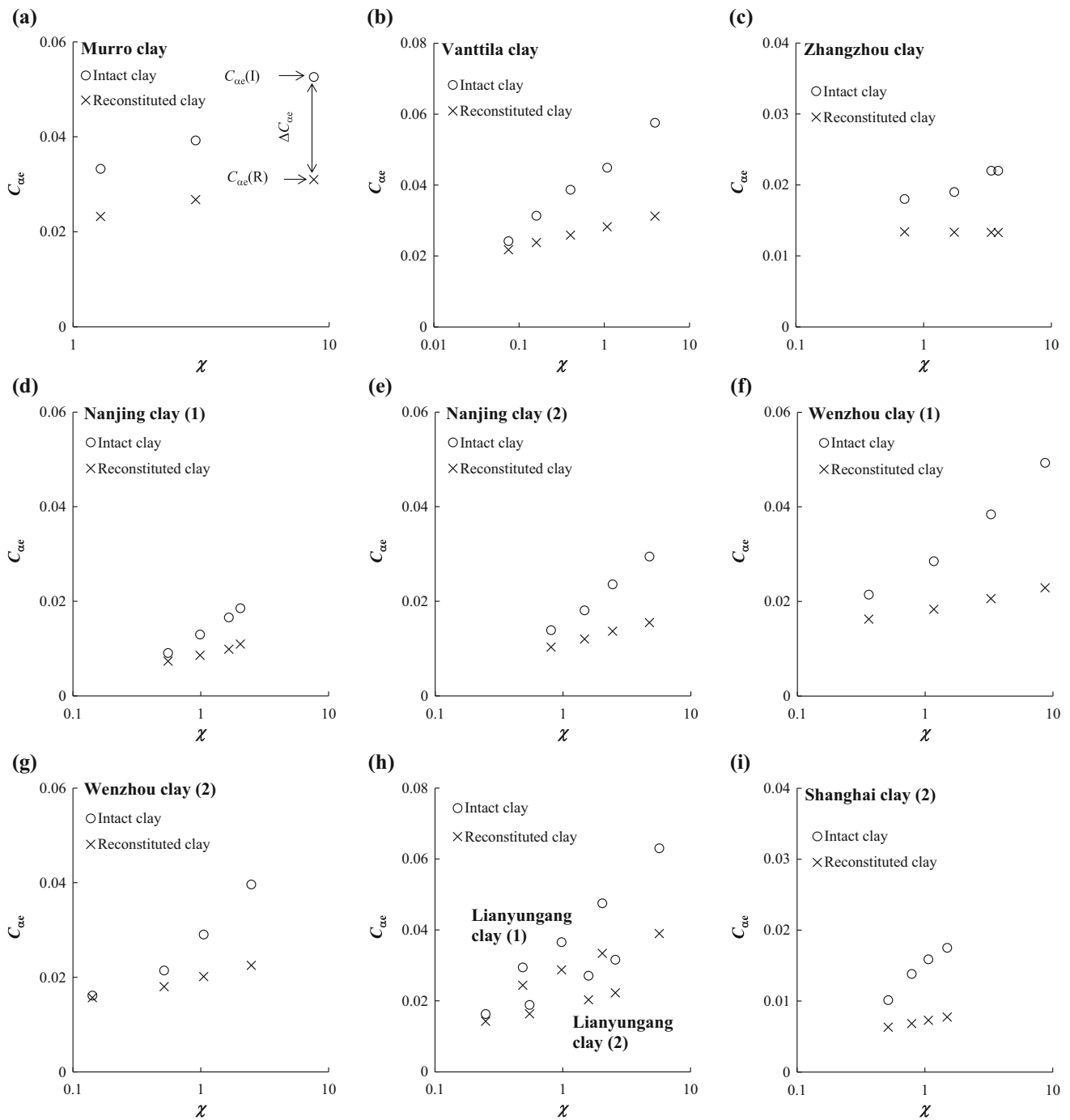


Fig. 4 Creep coefficient of intact and reconstituted clays versus bonding ratio

were selected. Figure 6a, b presents the plots of $C_{\alpha eL}$ with Atterberg limits, from which the following relation could be obtained with a correlation coefficient $R^2 = 0.9336$:

$$C_{\alpha eL} = 0.0007w_L - 0.0223 \tag{7}$$

Similarly, Fig. 6c, d shows the correlations for $C_{\alpha eP}$ indicating that the optimized correlation is obtained by using both the liquid limit and the plasticity index with a correlation coefficient $R^2 = 0.6913$:

$$C_{\alpha eP} = 0.0013w_L - 0.0013I_p - 0.0209 \tag{8}$$

From these correlations, it appears that the choice of $C_{\alpha eL}$ as the reference value for $C_{\alpha e}$ in Eqs. (2) and (6) is preferable given the higher correlation coefficient. Thus, the $C_{\alpha eL}$ with w_L can be used as reference in Eq. (6), and the Eq. (6) is rewritten as,

$$C_{\alpha e} = (n \log(\chi/\chi_0) + \rho_0 + 1)C_{\alpha eL}(w/w_L)^m \tag{9}$$

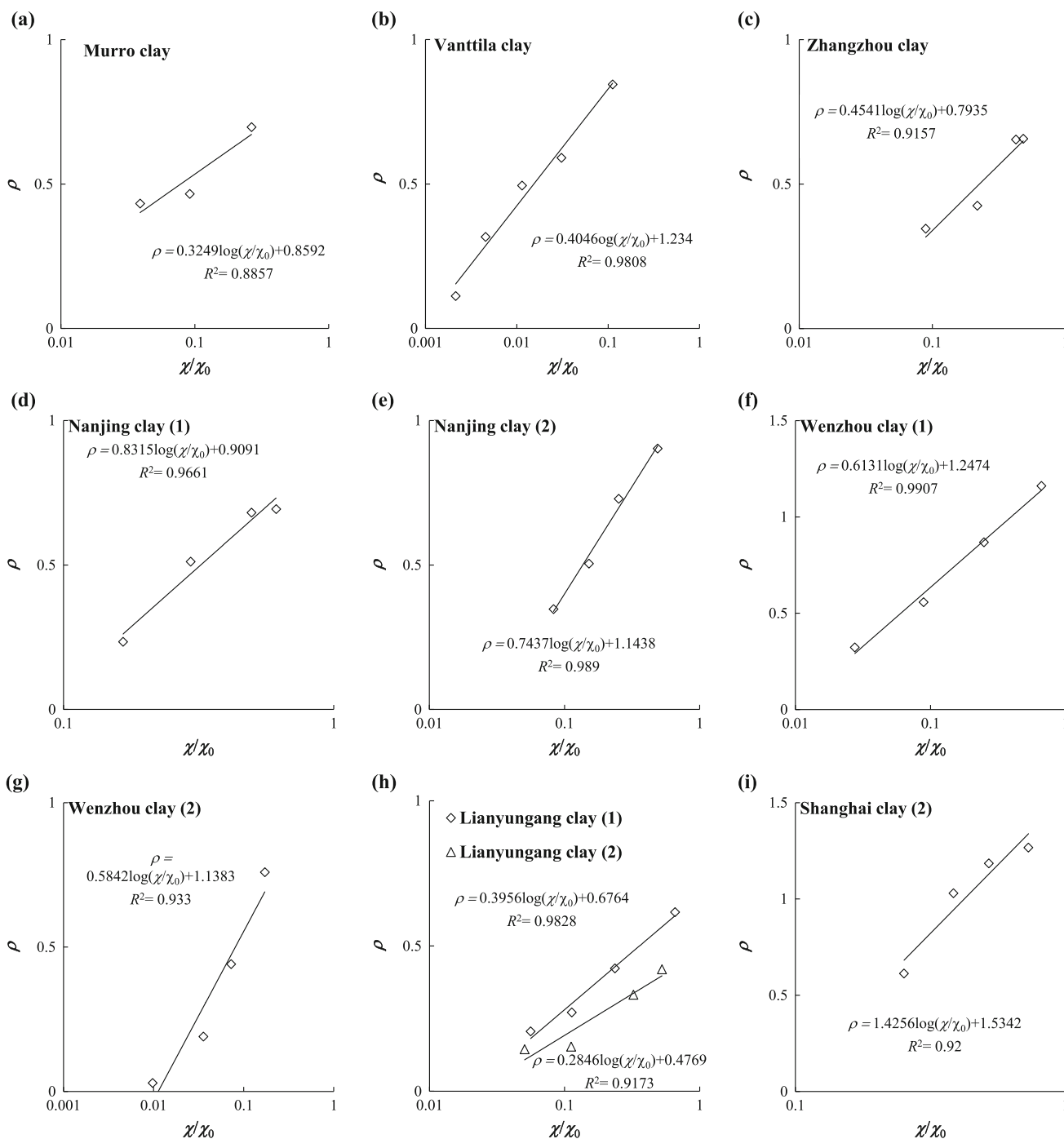


Fig. 5 Inter-particle debonding induced creep versus normalized bonding ratio

4.2 Correlation of *m* with Atterberg Limits

Based on all the estimated values of *m* shown in Eq. (6) for 15 reconstituted clays, the correlations between *m* and Atterberg limits were fitted. Figure 7 shows that the optimized correlation is obtained by using both liquid limit and plasticity index with a correlation coefficient $R^2 = 0.5217$:

$$m = 0.7872 - 0.0369w_L + 0.0619I_p. \tag{10}$$

4.3 Correlation of *n* with Atterberg Limits

Figure 8 presents the correlations between the material constant *n* shown in Eq. (6) and Atterberg limits based on test results on both intact and reconstituted samples of ten clays. It can be observed that the magnitude of *n* decreases

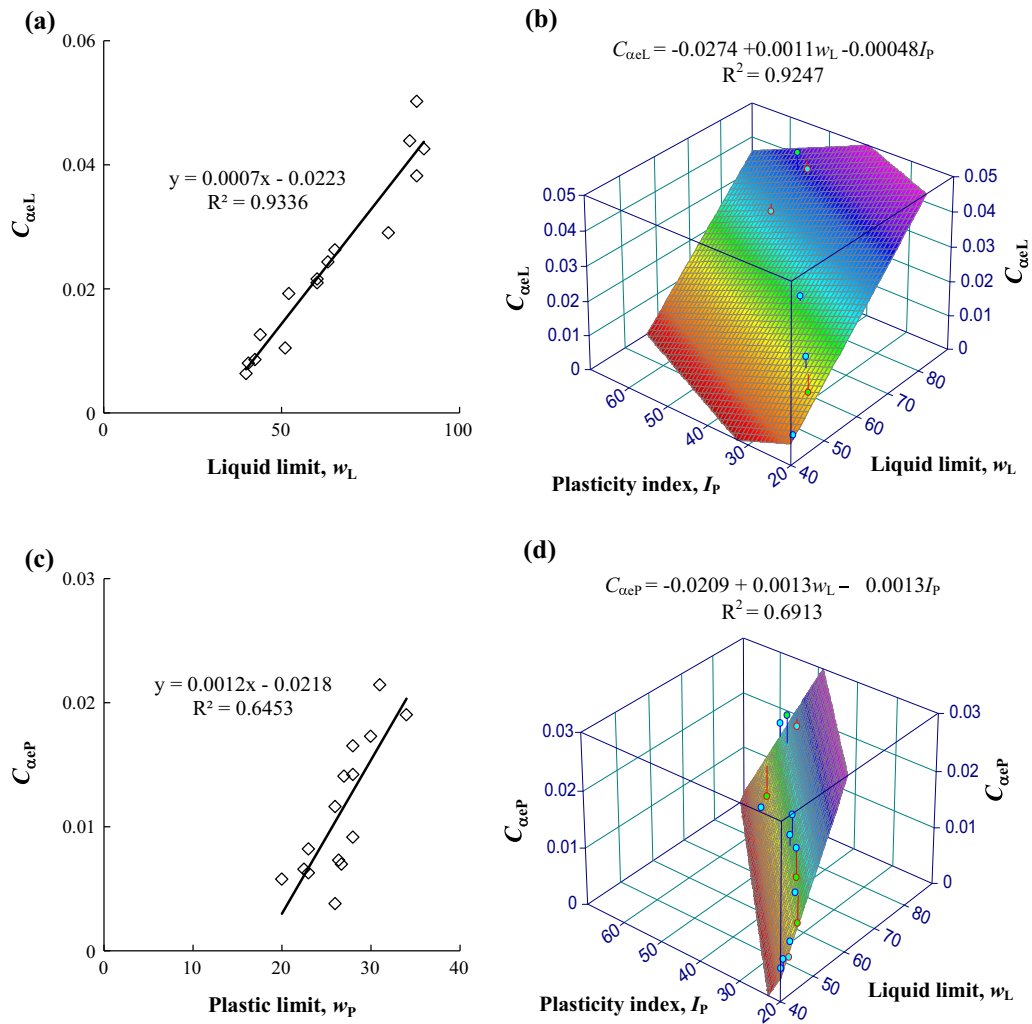


Fig. 6 Relationship between reference creep coefficients and Atterberg limits

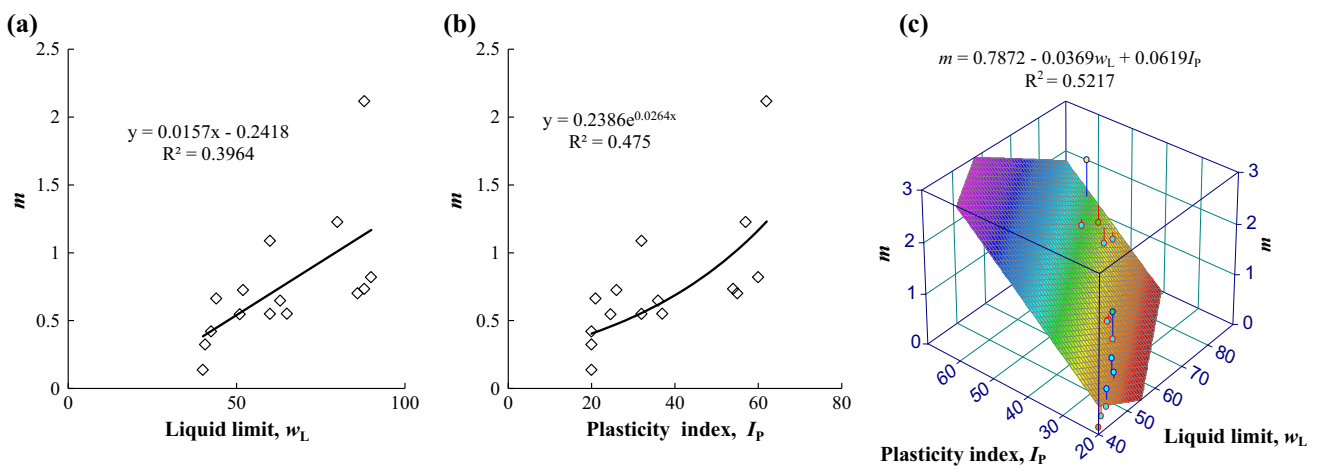


Fig. 7 Relationship between m and Atterberg limits

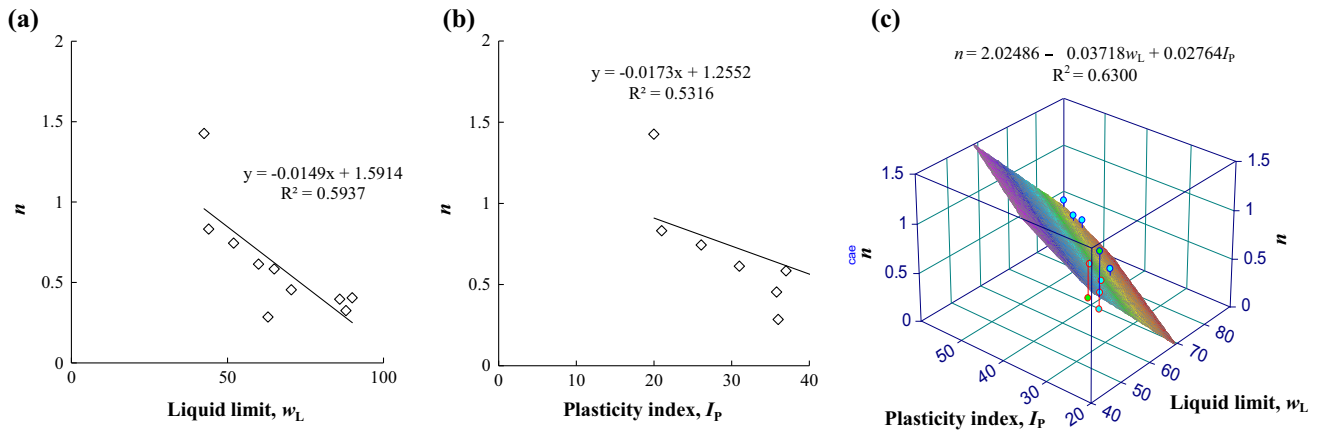


Fig. 8 Relationship between n and Atterberg limits

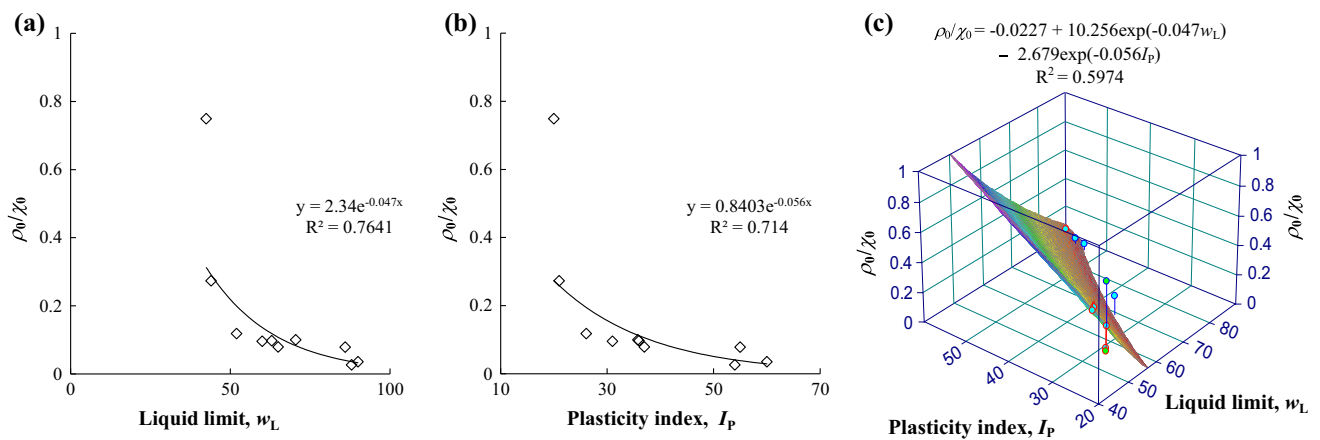


Fig. 9 Relationship between ratio ρ_0/χ_0 and Atterberg limits

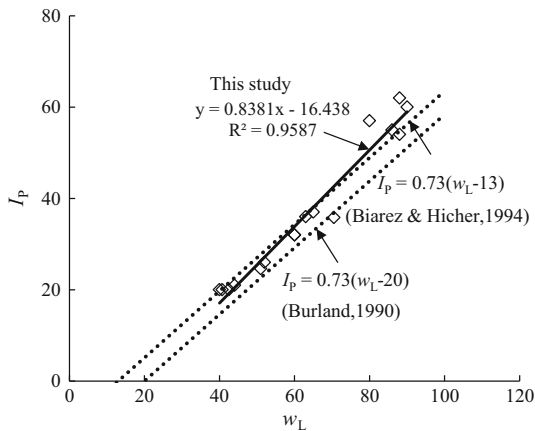


Fig. 10 Relationship between plasticity index and liquid limit

with the increase in the liquid limit or plasticity index. Furthermore, the values of n are shown to relate better with the liquid limit and plasticity index with a correlation coefficient $R^2 = 0.6300$:

$$n = 2.4630 - 0.0585w_L + 0.0532I_p. \tag{11}$$

4.4 Correlation of ρ_0 with Atterberg Limits

As mentioned above, ρ_0 is the initial value of ρ corresponding to $\chi = \chi_0$ and it represents the secondary compression potential induced by debonding. Consequently, a certain relation between ρ_0 and χ_0 can be observed. Hence, the link between the ratio ρ_0/χ_0 and Atterberg limits was analyzed from the test results on both intact and reconstituted samples of ten clays. Based on the findings, ρ_0/χ_0 can be expressed either by the liquid limit (Fig. 9a), or the plasticity index (Fig. 9b), or also by a unified expression with the liquid limit and the plasticity index (Fig. 9c). We adopted the latter expression with a correlation coefficient $R^2 = 0.7641$:

$$\rho_0/\chi_0 = 2.34 \exp(-0.047w_L) \tag{12}$$

5 Discussions

5.1 Correlation between I_p with w_L

A certain relationship between I_p and w_L is apparent. In the past, several expressions have been proposed such as the ones by Burland [4] with $I_p = 0.73(w_L - 20)$ and Biarez and Hicher [5] with $I_p = 0.73(w_L - 13)$. Figure 10 presents the plots of these two parameters for the clays

selected in this study together with the two lines representing the above correlations. The differences between these two lines and the experimental points are rather small, and we could consider one or the other correlation for our own materials. In order to remain as close as possible to our set of data, we chose to adopt the following best correlation represented in Fig. 10 by the bold line with a correlation coefficient $R^2 = 0.9587$:

$$I_p = 0.8381w_L - 16.438 \tag{13}$$

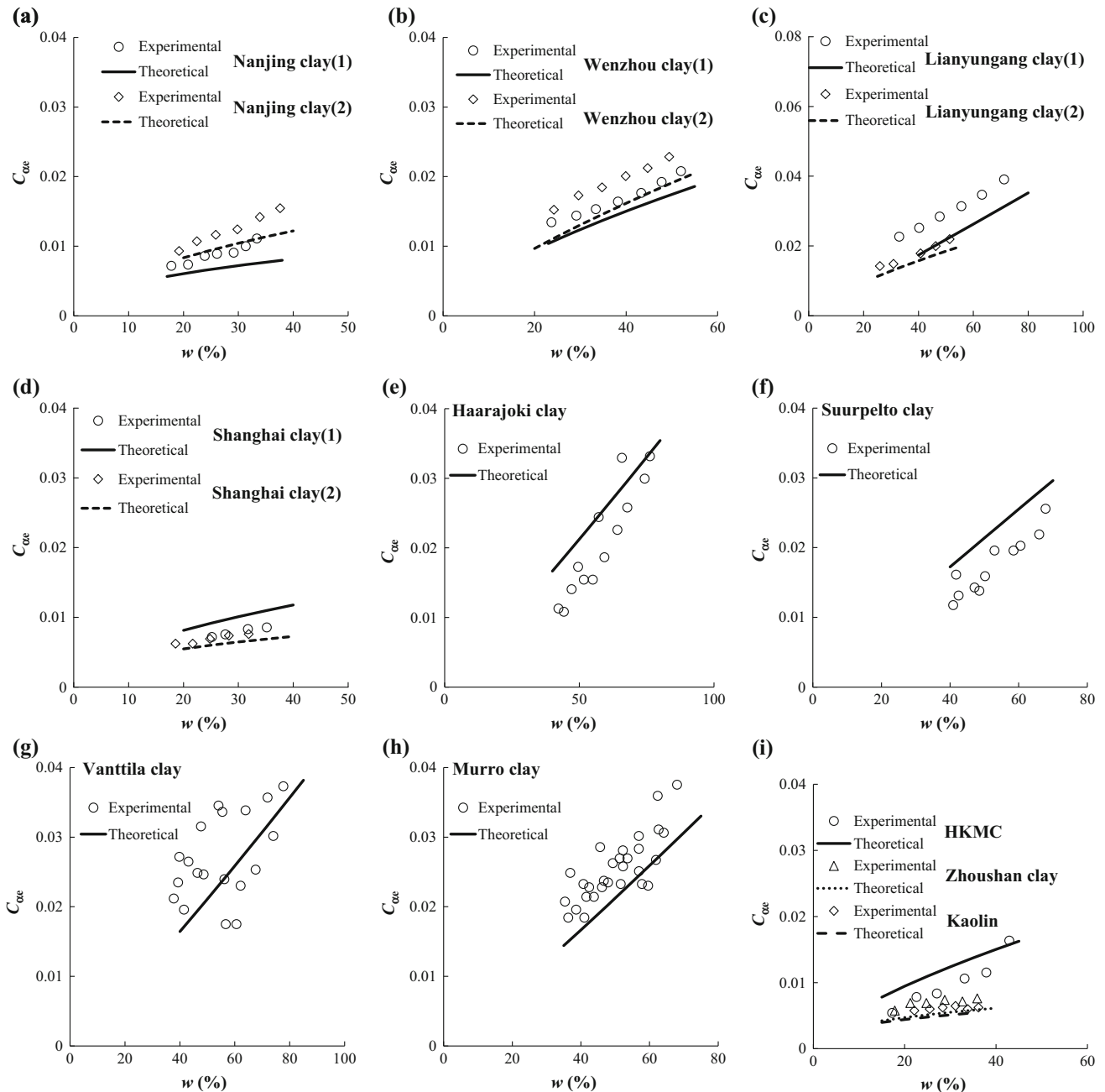


Fig. 11 Comparison of measured and estimated values of C_{oe} for reconstituted clays

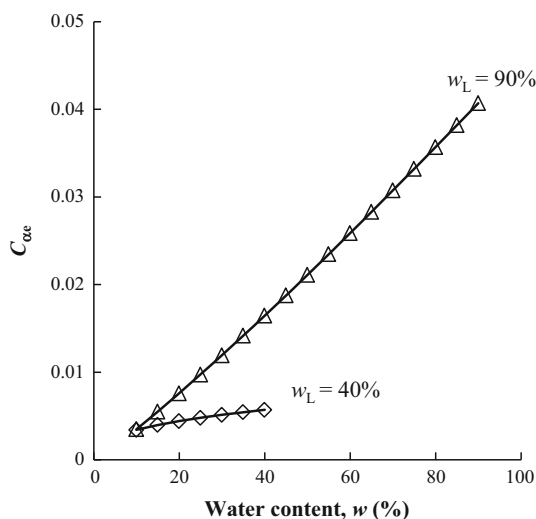


Fig. 12 Evolution of C_{oe} with water content for liquid limit equal to 40 and 90 %

Using Eq. (12), the above correlations of parameters with Atterberg limits can be simplified.

5.2 How to determine nonlinear creep

Over all, if the current water content (w), the bonding ratio (χ) and the liquid limit (w_L) of the clayey soil are known, the current C_{oe} can be obtained with the following process:

1. Substituting w_L into Eqs. (7), (12) and (13), C_{oeL} , ρ_0/χ_0 and I_p are obtained, respectively.
2. With w_L and I_p , m and n can be obtained by Eqs. (10) and (11), respectively.
3. The initial bonding ratio χ_0 can be taken equal to $(S_t - 1)$ according to Karstunen and Yin [10] and Yin et al. [32] with S_t the soil sensitivity, and then ρ_0 can be obtained since ρ_0/χ_0 is known from the first step of process.
4. Substituted all above correlated parameters into Eq. (9), C_{oe} is obtained.

Note that w and χ are two state variables representing current soil density and current soil structure, respectively. Thus, Eq. (9) accounts for the soil density and the soil structure during straining with clear physical meaning, and can be of practical use for determining simply the creep potential of a given natural soft clay.

5.3 Validation for reconstituted clays

For reconstituted clays, the structure between particles is eliminated; therefore, χ_0 can be regarded null. Consequently, a reduced form of Eq. (9) for reconstituted clays can be written as:

$$C_{oe} = (0.0007w_L - 0.0223)(w/w_L)^{0.014978w_L - 0.23031} \quad (14)$$

Figure 11 shows the comparison between experimental and predicted results estimated by Eq. (14) for all the selected clays. Despite there are some discrepancies between measured and estimated values, Eq. (14) generally describes the evolution of C_{oe} for reconstituted clays fairly well. We illustrated the influence of w_L on C_{oe} in Fig. 12. Because the maximum and minimum values of w_L in Table 1 are 90 and 40 %, we plotted the evolution of C_{oe} with water content for two clays having these liquid limits. It can be seen that the clay with a higher w_L presents a higher increasing rate and that C_{oe} decreases with the decreasing water content (i.e., decreasing void ratio) for each clay.

5.4 Validation for intact clays

For the ten intact clays shown in Fig. 4, the predicted values of C_{oe} were estimated by Eq. (9) with the liquid limit w_L and the structural parameter χ_0 listed in Table 2. Figure 13 compares experimental and predicted results in a 3D form ($C_{oe-w-\chi}$). It can be concluded that Eq. (9) is able to estimate with good accuracy the evolution of C_{oe} for the majority of the studied clays. For the others, even if differences between measured and estimated values still remain (e.g., Lianyungang clay), the trend is well captured.

Furthermore, the proposed formulation (Eq. 9) was examined on predicting the evolution of void ratio with time during creep. For this, long-term oedometer tests on Vanttila and Wenzhou intact clays, with strong and moderate level of soil structure, were selected. Only parts of curves apparently after consolidation or dissipation of excess pore pressure were plotted for both computed and measured results in Fig. 14. Curves by using constant C_{oeL} were also computed shown by dash lines for comparison. The computed void ratio by Eq. (9) decreases nonlinearly with time in logarithm scale for each loading shown by solid lines, which demonstrates that the proposed formulation can well capture the nonlinear creep degradation.

6 Conclusions

The one-dimensional creep characteristics of soft clays have been investigated based on experimental results from oedometer testing. The evolution of C_{oe} for reconstituted and intact clays was studied.

For reconstituted clays, the influence of the soil structure could be eliminated. A nonlinear creep behavior has been observed with C_{oe} decreasing when the soil density

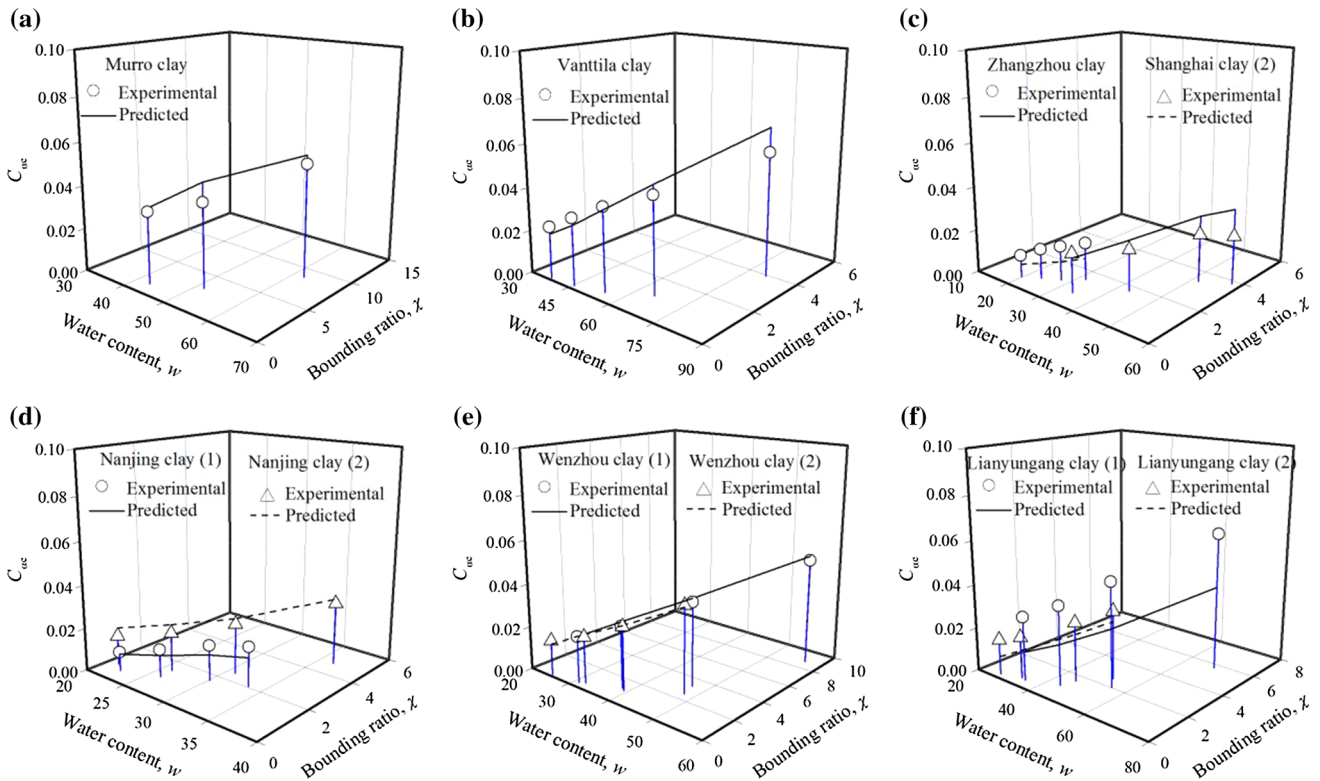


Fig. 13 Comparison of measured and estimated values of C_{oe} for intact clays

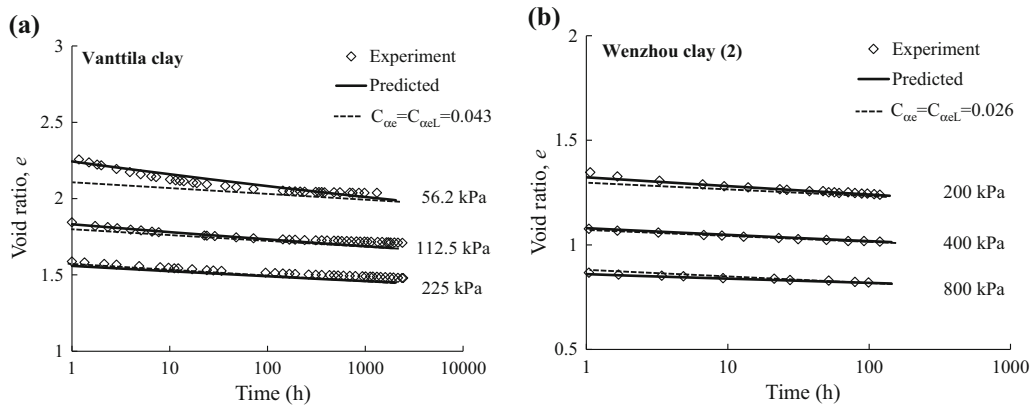


Fig. 14 Comparison of measured and computed void ratio versus time on two intact clays

increases. Based on these results, a simple nonlinear creep formulation was adopted with an additional parameter of nonlinearity m . For simplification and practical use, C_{oeL} (corresponding to the liquid limit) and C_{oeP} (corresponding to the plastic limit) were suggested as the reference C_{oe} .

The bond degradation process during straining exerts a significant influence on the values of C_{oe} . The significant difference of C_{oe} between intact and reconstituted clays was analyzed. The ratio of C_{oe} between intact clay and the corresponding value for reconstituted clay was related to

the bonding ratio with an additional parameter n , leading to a nonlinear creep formulation accounting for soil structure.

The proposed formulation of C_{oe} for intact clays contains five material constants C_{oeL} , C_{oeP} , m , n and ρ_0 , which can be determined in a straightforward way from conventional oedometer testing. Furthermore, correlations between these material parameters and Atterberg limits were proposed based on available data. By expressing the material constants as functions of the liquid limit and the plasticity index, we are able to suggest a practical

expression of $C_{\infty c}$ as a function of the current water content w , the bonding ratio and the physical properties of the clay. These correlations allow the determination of the material constants from the sole knowledge of the liquid limit of a given clayey soil. Its capacity of estimating the $C_{\infty c}$ values of various clays has been demonstrated, and accurate estimations of the one-dimensional creep characteristics of both reconstituted and natural soft clays were obtained. Furthermore, the proposed formulation is also validated by comparing the computed and measured void ratio with time on two intact clays.

This study provides a simple way of estimating the creep coefficient of natural clays, which can be of practical use in geotechnical engineering. Since it is a key parameter for many creep modeling approaches, the creep coefficient can be used as a state variable based on this study and applied to a framework of modern and full-edged constitutive description in future studies, along with the modeling of the consolidation phase.

Acknowledgments We acknowledge with gratitude the financial support provided by the National Natural Science Foundation of China (Grant No. 41372285), the Fundamental Research Funds for the Central Universities in China (2015QNA64) and the European project CREEP (PIAPP-GA-2011-286397).

References

- Adachi T, Oka F (1982) Constitutive equations for normally consolidated clay based on elasto-viscoplasticity. *Soils Found* 22(4):57–70
- Augustesen A, Liingaard M, Lade PV (2004) Evaluation of time-dependent behavior of soils. *Int J Geomech* 4(3):137–156
- Bjerrum L (1967) Engineering geology of Norwegian normally-consolidated marine clays as related to settlements of building. *Géotechnique* 17(2):81–118
- Burland JB (1990) On the compressibility and shear strength of natural clays. *Géotechnique* 40(3):329–378
- Biarez J, Hicher PY (1994) Elementary mechanics of soil behaviour. Balkema, Boca Raton
- Chen XP, Zeng LL, Lü J, Qian H, Kuang LW (2008) Experimental study of mechanical behavior of structured clay. *Rock Soil Mech* 29(12):3223–3228
- Desai DS, Sane S, Jenson J (2011) Constitutive modeling including creep- and rate-dependent behavior and testing of glacial tills for prediction of motion of glaciers. *Int J Geomech* 11(6):465–476
- Gens A, Nova R (1993) Conceptual bases for a constitutive model for bonded soils and weak rocks. In: Proceedings of international symposium on hard soils–soft rocks, Athens, pp 485–494
- Graham J, Crooks JHA, Bell AL (1983) Time effects on the stress-strain behaviour of natural soft clays. *Géotechnique* 33(3):327–340
- Karstunen M, Yin Z-Y (2010) Modelling time-dependent behaviour of Murro test embankment. *Géotechnique* 60(10):735–749
- Kutter BL, Sathialingam N (1992) Elastic-viscoplastic modelling of the rate-dependent behaviour of clays. *Géotechnique* 42(3):427–441
- Leoni M, Karstunen M, Vermeer PA (2008) Anisotropic creep model for soft soils. *Géotechnique* 58(3):215–226
- Leroueil S, Kabbaj M (1987) Discussion on ‘Composition and compressibility of typical samples of Mexico City clay’ by Mesri et al. *J Geotech Eng Div* 113(9):1067–1070
- Leroueil S, Kabbaj M, Tavenas F (1988) Study of the validity of a $\sigma'_v - \varepsilon_v - \dot{\varepsilon}_v$ model in in situ conditions. *Soils Found* 28(3):13–25
- Leroueil S, Kabbaj M, Tavenas F, Bouchard R (1985) Stress–strain–strain rate relation for the compressibility of sensitive natural clays. *Géotechnique* 35(2):159–180
- Li Q, Ng CWW, Liu G (2012) Low secondary compressibility and shear strength of Shanghai clay. *J Cent South Univ* 19(8):2323–2332
- Mesri G, Godlewski P (1977) Time and stress-compressibility interrelationship. *J Geotech Eng Div* 103(5):417–430
- Mitchell JK, Soga K (2005) Fundamentals of soil behavior. Wiley, New York
- Niemunis A, Grandas-Tavera CE, Prada-Sarmiento LF (2009) Anisotropic visco-hypoplasticity. *Acta Geotech* 4:293–314
- Nagaraj TS, Srinivasa Murthy BR (1983) Rationalization of Skempton’s compressibility equation. *Géotechnique* 33(40):433–443
- Nagaraj TS, Pandian NS, Narasimha Raju PSR, Vishnu Bhushan T (1995) Stress-state-time permeability relationships for saturated soils. In: Proceedings of the International symposium on compression and consolidation of clayey soils is–Hiroshima, Japan, pp 537–542
- Nash DFT, Sills GC, Davison LR (1992) One-dimensional consolidation testing of soft clay from Bothkennar. *Géotechnique* 42(2):241–256
- Smith PR, Jardine RJ, Hight DW (1992) On the yielding of Bothkennar clay. *Géotechnique* 42(2):257–274
- Stapelfeldt T, Lojander M, Vepsäläinen P (2007) Determination of horizontal permeability of soft clay. In: Proceeding of the 17th international conference of soil mechanics and foundations, vol 3, Madrid, pp 1385–1389
- Suneel M, Park LK, Im JC (2008) Compressibility characteristics of Korean marine clay. *Mar Georesour Geotechnol* 26:111–127
- Vermeer PA, Neher HP (1999) A soft soil model that accounts for creep. In: Proceedings Plaxis symposium “beyond 2000 in computational geotechnics”, Amsterdam, pp 249–262
- Yin JH (1999) Non-linear creep of soils in oedometer tests. *Géotechnique* 49(5):699–707
- Yin J (2015) Fundamental issues of elastic viscoplastic modelling of the time-dependent stress–strain behavior of geomaterials. *Int J Geomech*. doi:10.1061/(ASCE)GM.1943-5622.0000485
- Yin JH, Graham J (1989) Viscous elastic plastic modelling of one-dimensional time dependent behavior of clays. *Can Geotech J* 26:199–209
- Yin JH, Zhu JG, Graham J (2002) A new elastic viscoplastic model for time-dependent behaviour of normally and overconsolidated clays: theory and verification. *Can Geotech J* 39:157–173
- Yin ZY, Hicher PY (2008) Identifying parameters controlling soil delayed behaviour from laboratory and in situ pressuremeter testing. *Int J Numer Anal Methods Geomech* 32(12):1515–1535
- Yin ZY, Chang CS, Karstunen M, Hicher PY (2010) An anisotropic elastic viscoplastic model for soft soils. *Int J Solids Struct* 47(5):665–677
- Yin ZY, Karstunen M, Chang CS, Koskinen M, Lojander M (2011) Modeling time-dependent behavior of soft sensitive clay. *J Geotech Geoenviron Eng* 137(11):1103–1113
- Yin ZY, Xu Q, Yu C (2012) Elastic viscoplastic modeling for natural soft clays considering nonlinear creep. *Int J Geomech*. doi:10.1061/(ASCE)GM.1943-5622.0000284

35. Yu XJ, Yin ZZ, Dong WJ (2007) Influence of load on secondary consolidation deformation of soft soils. *Chin J Geotech Eng* 29(6):913–916
36. Zeng LL, Hong ZS, Liu SY, Chen FQ (2012) Variation law and quantitative evaluation of secondary consolidation behavior for remolded clays. *Chin J Geotech Eng* 34(8):1496–1500
37. Zhang XW, Wang CM (2012) Effect of soft clay structure on secondary consolidation coefficient. *Rock Soil Mech* 33(2):476–482